Article

Pesticide-Free Robotic Control of Agricultural Pests

Virginie Lacotte [1], Toan NGuyen [2], Javier Diaz Sempere [2], Vivien Novales [2], Vincent Dufour [2], Richard Moreau [2], Minh Tu Pham [2], Kanty Rabenorosoa [3], Sergio Peignier [1], François G. Feugier [4], Robin Gaetani [4,5], Thomas Grenier [6], Bruno Masenelli [5], Pedro Da Silva [1], Abdelaziz Heddi [1] and Arnaud Lelevé [2]*

1   INSA Lyon, INRAE, BF2I, UMR 203, Univ Lyon, 69621 Villeurbanne, France; pedro.da-silva@insa-lyon.fr
2   Univ Lyon, INSA Lyon, Université Claude Bernard Lyon 1, Ecole Centrale de Lyon, CNRS, Ampère, UMR5005, 69621 Villeurbanne, France; arnaud.leleve@insa-lyon.fr
3   FEMTO-ST, UBCF, CNRS, France; rkanty@femto-st.fr
4   Greenshield Technologies, France; francois.feugier@greenshield.com
5   Univ Lyon, INSA Lyon, CNRS, Ecole Centrale de Lyon, Université Claude Bernard Lyon 1, CPE Lyon, INL, UMR5270, 69621 Villeurbanne, France; bruno.masenelli@insa-lyon.fr
6   Univ Lyon, INSA-Lyon, Université Claude Bernard Lyon 1, UJM-Saint Etienne, CNRS, Inserm, CREATIS UMR 5220, U1294, F-69100, Lyon, France; thomas.grenier@creatis.insa-lyon.fr
*   Correspondence: arnaud.leleve@insa-lyon.fr

Abstract: Because our civilization has relied on pesticides to fight weeds, insects, and diseases since Antiquity, the use of these chemicals has become natural and exclusive. Unfortunately, the use of pesticides has progressively had alarming effects on water quality, biodiversity, and human health. This paper proposes to improve farming practices by replacing pesticides with a laser-based robotic approach. This study focused on the neutralization of aphids as they are among the most harmful pests for crops and complex to control. With the help of deep learning, we developed a mobile robot that spans crop rows, locates aphids, and neutralizes them with laser beams. We have built a prototype with the only purpose to validate the localization-neutralization loop on a single seedlings row. The experiments performed in our laboratory demonstrate the feasibility of detecting different lines of aphids (50% detected at 3 cm/s) and of neutralizing them (90% mortality) without impacting the growth of their host plants. The results are encouraging since aphids are one of the most challenging crop pests to eradicate. However, enhancements in detection and mainly in targeting are necessary to be useful in a real farming context. Moreover, robustness regarding field conditions should be evaluated.

Keywords: Farming; Robotics; Aphid Detection; Laser-based Neutralization; Deep Learning; Image Based Visual Servoing

1. Introduction

The use of pesticides has become natural and exclusive to us because our civilization has relied on them since Antiquity to fight weeds, insects, and diseases, which would generate a mean 50% production loss [1]. Unfortunately, this has progressively led to alarming consequences on water quality, biodiversity, and human health. Exposure of the European population to endocrine-disrupting pesticides alone cost up to €270B in health expenses in 2017 [2]. Tang *et.al* [3] concluded that 64% of global agricultural land ($25.106 km^2$) is at risk of pesticide pollution, and 31% is at high risk. The class of neonicotinoids, pesticides responsible for the deaths of 300,000 bee colonies annually, has even been recently banned from use [4]. In its "Ecophyto" plan, the French government has decided to reduce by 50% the use of agrochemicals by 2018. Unfortunately, alternatives to chemicals being too scarce, the objective has been postponed to 2025.

For ten years, progress in computer science, robotics, and agronomic modes have improved farming practices, provoking two consecutive revolutions: the smart [5] and today, the robotic farming [6]. Spectral analysis solutions are henceforth used for pests

and diseases monitoring on crops [7,8], detection of insect infestations on stored grains, mosquito gender and age evaluation, and taxonomical applications [9], with excellent results. The detection performed with 3D cameras, a computer-based classification, and notably, deep learning algorithms [10–12] has also been investigated. However, very few works are held on laser-based neutralization of insect pests as an alternative to pesticides. Besides, weed processing is now actively commercialized [13]. The destruction is typically targeted-herbicide-spray or mechanically based, sometimes thermal, but laser-based destruction is also still under study [14]. As soon as 2001, laser-burning could reduce their biomass by 90% with only 20% of the energy usually used for thermal weeding [15].

To date, technologies for automated spraying or mechanical destruction of weeds are appearing on the market either as large and costly farming robots [16] or as small-sized ones, such as Oz (Naïo Tech). Yet, no non-chemical solution exists concerning crop pests. This is why the Greenshield[1] objective was to demonstrate the feasibility on aphids of a laser-based Detection-Neutralisation Module (DNM) embedded in a custom mobile robot. It managed to do it in lab conditions in September 2021. It also demonstrated the feasibility on weeds of the DNM embarked on a commercially available robot (Dino, Naio Tech).

Detecting aphids in crop fields is a complex task due to their small size and confounding color. As for numerous other applications, a Deep Learning approach has been envisaged. Indeed, this Artificial Intelligence approach is nowadays widespread for face recognition [17], image segmentation [18], signal analysis and automatic interpretation, or the control of autonomous cars. More particularly, deep learning and image processing are two disciplines whose applications are very varied and encompass areas such as medicine, robotics, security, and surveillance. In the field of image processing, deep learning is very powerful to extract complex information from input images. Such algorithms' structures are often based on convolutional neural networks that can capture the spatial dependencies at a different scale in an image. They consist of stacking of layers of convolution and mathematical functions with several adjustable parameters, which seek to identify the presence of particular patterns on the image at different scales. The tuning and the optimization of these parameters are performed during a preliminary training phase, which relies on the availability of a large quantity of data, thanks to specific cost functions (loss).

The originality of this project lies in the embedding of various technologies in a single farming robot necessitating a multidisciplinary including pest biology, laser photonics, visual servoing, and mobile robotics. This paper is organized as follows. Next section details materials and methods for detection and neutralization. Experimental results are provided in Section 3 and discussed in Section 4. We then conclude this paper which summarizes the achievements of the Greenshield project, and we evoke future directions.

2. Materials and Methods

The study focused on the neutralization of aphids as they are among the most harmful pests for crops and complex to control [19]. To do so, we chose three aphid lines different in color and size, providing a diverse database to develop our DNM. Thus, we used two pea aphid lines, *Acyrthosiphon pisum* LL01 (green) and YR2 (pink), and one bird cherry-oat aphid line *Rhopalosiphum adi* LR01 (black, 2 to 3 times smaller than *A. pisum*). A solution able to control their spreading should work more likely on other invertebrates such as cockroaches, mosquitoes, fruit flies, and floor beetles.

A trolley-like robot embedding three subsystems is proposed: the RGB-D (Red-Green-Blue plus Depth) acquisition system and light sources, the aphids localization algorithm using deep learning, and the neutralization system based on the laser. Figure 1 illustrates the whole system organization inside the robot.

The light sources, the camera, and the seedlings featuring several aphids were collocated into a black box.

---

1 See https://anr-greenshield.org

In the following, we detail each subsystem and start with a global overview of the neutralization process.
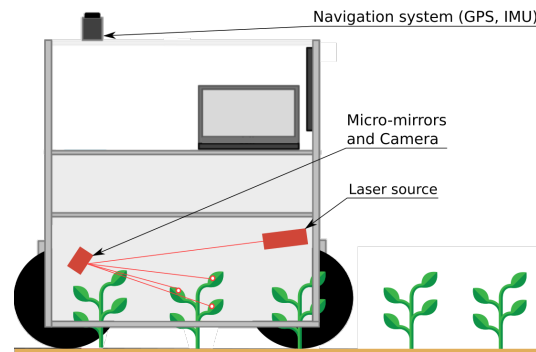

Figure 1. Greenshield prototype description and working principle: the robot spans a crop row, detects the aphids on leaves, and targets them using the laser beam positioned by the micro-mirrors.

2.1. Global process

The mobile robot spans plant rows one by one. When a plant is detected, the robot stops, and then aphid detection and neutralization tasks start. For the real-time detection of aphids, we use a 3D camera and Artificial Intelligence object recognition techniques (Section 2.3). The coordinates of the aphids visible on each image are transmitted to the neutralization module.

The aphid neutralization module is mounted on the robot and consists of a (harmless) laser pointer and a power laser source, taking the same optical path toward a pair of micro-mirrors (see Fig. 2b) that position beams in the robot's workspace (see Fig. 1). The laser pointer is used to realize a visual servoing (detailed in Section 2.4.1) to target the aphids located in the camera images. Once the pointer spot is stabilized on the target, the power laser emits a pulse carrying a sufficient amount of energy to neutralize the target aphid (by raising its temperature, see Section 2.5). It then moves on to the next targeted aphid in the image. When all detected aphids are treated, the robot moves again until a new plant is detected. Several types of low-power laser sources that can be mounted on a mobile robot have been tested to identify the best beam tracking on the leaves. Experiments were performed allowing us to correlate the energy emitted by the laser beam with the fecundity and mortality rates of aphids and the efficiency of weed destruction. The detection/localization/neutralization software was linked to the robot locomotion to dynamically enable proceeding. ROS middleware was used to manage the communication between modules.

(a) ZED mini camera (stereo labs).
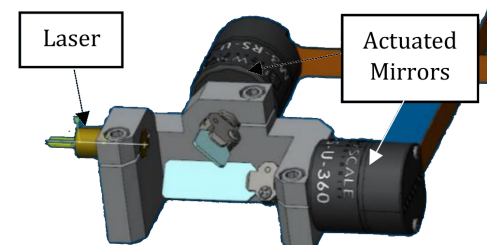
(b) 2 degrees of freedom actuated mirrors for laser positioning (DK-M3-RS-U-2M-20-L, Newscale Technology).

Figure 2. Camera and laser steering device.

2.2. Image acquisition

To localize aphids, the RGB-D camera ZED mini camera (Stereo labs[2] is used (see figure 2a). Its settings were adjusted to limit light reflections and maximize the contrast (maximum contrast and saturation, reduced gain, see table 1) to ensure the best image acquisition in the lighting condition.

The light sources used are white LEDs, and, to reduce the impact of the foreign light sources, we added some light protections as can be observed in figure 7. These protections will also serve to limit laser exposure.

Table 1. Configuration of various parameters of the ZED camera.

Parameters	Values	Explanation
Resolution	HD1080 (1920x1080)	A 2K resolution would consume a lot of resources and therefore would slow down the detection algorithm.
Capture Speed	30 FPS	Maximum available in the HD1080 mode
Brightness	1	Low brightness to limit light reflections on the surface of the leaves.
Contrast	6	High contrast makes it easier to detect pink aphids on green leaves.
Hue	0	Default value, that matches the colors perceived by human eyes.
Saturation	8	Maximized to let the aphids appear on green leaves.
Gamma	2	A low gamma level limits the white light in the picture.
Acuity	4	Average value as high values generate noise on the back plane.
White Balance	auto	To adapt it taking into account fixed other color parameters (hue, saturation).
Exposition	75%	Set to keep the brightness at an acceptable level.
Gain	10	Adjusted to keep the consistency between the other settings with minimal add noise addition.

2.3. Detection and Localization

The objective of this module is to detect aphids on images of crops that the robot scans over, localize them, and send these coordinates to the neutralization module described below. In terms of specifications, it must meet the following three criteria:

- detection accuracy: a maximum error of 3 mm between the center of detected aphids and their localization in the image;
- detection sensitivity: at least 60% of aphids present in the image[3];
- real-time operation: the entire program (detection algorithm + laser control) must run at a speed greater than 10 frames per second to permit the robot to cover a 1ha crop field in 24h[4].

The problem of detecting and localizing aphids of different sizes, colors and positions in natural image sequences of various crops is particularly difficult. From our knowledge, only artificial neural networks based on deep learning detection architectures can perform this task in real-time. Therefore, to detect aphids in each image acquired by the camera located under the robot as the latter proceeds over each crop row, we selected from the current arsenal of detection architectures (EfficientDet, Yolo, FasterRCNN, Unet+Hausdorff), the YOLO version 4 [20] for its speed and its small size object performance in images. Such approaches are supervised, this means that an important data set with manual annotations is needed for the training phase. When trained, the network is transferred and run on an embedded GPU board (Nvidia Jetson Xavier AGX).

---

[2] See https://www.stereolabs.com/zed-mini/

[3] This level has been set arbitrarily taking into account that natural predators should finish the work, but it requires experimental validation.

[4] In the case of a field where rows are located every 40cm, the robot will have to travel 25km during 12h, corresponding to a mean speed of 1km/h or 29cm/s.

To do that, we first built an image database featuring aphids on broad bean seedlings. The training set of images was annotated using *labelme*[5] software. Around 700 images were labeled, featuring each one with 20 to 30 aphids. It was necessary to manually draw a bounding box around each aphid as well as to put a dot on the center of each aphid. Since we did not have a sufficient amount of images for training the neural nets, we applied data augmentation on these images to avoid the phenomenon of overfitting and improve the generalization ability of the trained model to new images. The following image transformations were applied randomly to generate modified images during training:

- Horizontal or vertical image flip
- Rotation of 10° in the positive or negative direction
- Brightness modification
- Hue and saturation modification
- Contrast modification
- Grayscale modification

We started to develop this localization function with a YOLOv4[6] as it is very efficient in the detection of objects in real-time, and is broadly used in applications requiring fast detection speed as for drones or autonomous car vision. YOLOv4 is a one-stage detector. Its backbone is CSPDarknet53 [21], a model tuned for image recognition. Darknet has been designed to diminish the issues of gradient loss[7], encourage the network to reuse feature maps (with residual layers), and reduce the set of optimization parameters. The secondary part of the network (the neck) features a PANet (Path Aggregation Network) [22] to mix and combine the maps of characteristics generated by the backbone. It is indeed a preparation step for the following detection. The YOLO detector can predict the class of the object, its bounding box, and the probability of its presence in its bounding box. Nevertheless, because of its small characteristic maps, this kind of multi-scale detector struggles to detect small objects in the image. Thus, in practice, it could not detect aphids located at a distance greater than 30cm from the camera. We tested several input image sizes (640x640 and 512x512) knowing that the size of the images acquired by the camera is 2208x1242 pixels, to determine the best choice. We also optimized the network process using batch inference, which was not yet implemented in the original YOLOv4 code. We chose tkDNN[8], which is a neural network library specifically designed to work on NVIDIA Jetson boards. It is built with the primitives of cuDNN, a library from NVIDIA regarding neural networks, and TensorRT, an inference platform high performance that enables high throughput and low latency for inference applications related to deep learning. TensorRT engine optimizes models by quantifying all network layer parameters and converting them into formats that occupy less memory space. The tkDNN library allows inference with network parameters in three different formats: FP32, FP16, and INT8. In this project, we chose the FP16 format as it is displayed as the most accurate and efficient format [9]. The data degradation caused by format conversion remains meaner than 0.02%.

We also studied an approach to detect smaller objects, without a bounding box and based on the weighted distance of Hausdorff[10]. The chosen architecture was a U-Net optimized with a loss function based on this distance. Rather than taking bounding boxes as references (ground truth), the network seeks to localize objects according to reference points. The issue with this network in our application is that the clustering method requires exact information on the number of aphids present in the image. When the number of aphids or the number of clusters on the image is not well estimated by the output of regression, this risks mislocating centroids and in this case, the detection will have no

---

5   See https://github.com/wkentaro/labelme
6   Whose code is available on https://github.com/AlexeyAB/darknet
7   See Vanishing Gradient Problem and Solutions: https://deepai.org/machine-learning-glossary-and-terms/vanishing-gradient-problem
8   The source code for tkDNN is available on Github: https://github.com/ceccocats/tkDNN
9   See https://github.com/ceccocats/tkDNN#fps-results
10   Code available on Github: https://github.com/javiribera/locating-objects-without-bboxes

interest. We searched for a method that determines the centroids without estimating the number of objects. So, we disabled the regression layers in U-Net and we used the DBScan method instead of the Gaussian Mixture [23] to determine the points of interest. It also reduces the number of parameters of the network, which makes the model more suitable for the limited GPU resources of Nvidia Jetson boards. However, the use of DBScan risked generating many disturbances if the images were not correctly segmented. Post-processing was then relevant to filter noise. Once the points were well located on the image in the form of pixel coordinates, it was then possible to convert these points into a 3D reference using the Software Development Kit of the ZED mini camera. Indeed, the 2D image is taken only by one of the two objectives of the ZED camera, and the other is used to interpret the points in 3 dimensions. As the captured images are in RGBXYZ format (2D image with depth), we could obtain the cloud measurement of neighborhood points in XYZ (3D) from a detected point on the RGB (2D) image. The coordinates of the detected 3D point are therefore calculated as the median of this point cloud.

We evaluated the performance of these two convolutional neural networks (Darknet YoloV4 and UNet Hausdorff) using precision and recall criteria. Accuracy is defined by the proportion of correct detection among all the proposed detected aphids. Recall (or sensitivity) is the proportion of correct detection among all the relevant elements. A detection was considered a true positive when the distance between its predicted position and the reference was less than 5 pixels. This tolerance was defined by considering that the average size of aphids on the image was 10x10 pixels. This corresponds to a maximum error of 2mm when the aphids are close to the camera ($\approx$25cm) and 4mm when they are at the camera detection limit ($\approx$50cm). Both algorithms have been evaluated based on data from aphids that we acquired with 400 training images, 200 validation images, and 84 test images. The network was trained with the training, and validation images first. It was then evaluated with the other 84 images in the inference phase.

2.4. Laser-based Neutralization

2.4.1. Laser-based Targeting

Targeting aphids from their localization in acquired images requires visual servoing. Several works have dealt with this issue. The closer ones are analyzed here. In 1996, Hutchinson *et al.* proposed an IBVS (Image-Based Visual Servo) approach with a PID control law. They could obtain a mean and maximum error of 2 and 3 pixels respectively on flying mosquito targets [24]. In 2016, Andreff *et al.* used the same IBVS approach in laser micro-surgery, using also a 2DOF piezoelectric mirror to steer the laser ray [25], with a simple proportional gain in the control law, resulting in an exponential convergence of the error. In 2018, Kudryavtsev *et al.* developed a visual servoing system for a three-tube concentric tube robot, using an adaptive proportional gain approach that was successfully validated in simulation using the visual servoing platform ViSP and then in an experimental setup [26]. The adaptive gain increased the convergence speed while ensuring stability, avoiding overshoot for small errors and limiting the maximum speed.

Finally, we based this study on the works described in [27]. In this specific case, the system consisted of a coarse tracking system using a pair of stereoscopic cameras to identify the approximate 3D location of a mosquito pest target, to then implement a visual servoing system using a single high-speed camera and a fast scanning mirror to guide the tracking laser to the target pest through the minimization of a pixel tracking error. The annihilating laser dose was then administrated through the same optical path. To orientate the laser beams towards the targets, we chose a 2-axis system that orientates two micro-mirrors and permits $\pm$25° of rotation range with a resolution meaner than 5μrad in closed-loop and repeatability of 100μrad. This system features sensors with a bandwidth of 350 Hz for rotations meaner than 0.1°. The IBVS approach was chosen because of the properties of the laser-mirror system and the robot operation. The exact geometric relationship between the target and the mirrors is not known given the evident variability of the pest locations and the complicated potential estimation of their 3D position using the camera, in contrast to
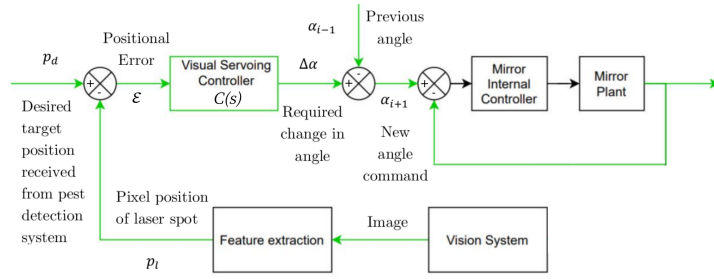
Figure 3. Control scheme with visual servoing.

an industrial application where the target can be fixed. Three control laws were studied, consisting of two variants of an Adaptive Proportional Gain (AG1 and AG2), and a PID. These control laws were implemented in the Visual Servoing Controller in Fig. 3. The PID controller, expressed in z space, was:

$$C_{PID}(z) = K_p + K_i \frac{T}{1 - z^{-1}} + K_d \frac{1 - z^{-1}}{T} \tag{1}$$

where K_p, K_i, and K_d are constant parameters, and T is the sampling period. The AG1 controller was:

$$C_{AG1}[k] = \lambda[k] \quad \text{with} \quad \lambda[k] = \lambda[k-1] + c_1.e^{-c_2.\varepsilon[k]^2} \tag{2}$$

where $\lambda[k]$ is the adaptive gain, c_1 and c_2 constant parameters, and $\varepsilon[k]$ is the error signal ($\varepsilon = p_d - p_l$). The AG2 controller was:

$$C_{AG2}[k] = \lambda[k] \quad \text{with} \quad \lambda[k] = (\lambda_0 - \lambda_\infty).e^{-\frac{\dot{\lambda}_0}{\lambda_0 - \lambda_\infty}\varepsilon[k]^2} + \lambda_\infty \tag{3}$$

where λ_0 (resp. λ_∞) is the gain when $\varepsilon = 0$ (resp. ∞), and $\dot{\lambda}_0$ the slope of $\lambda(\varepsilon)$ when $\varepsilon = 0$ [28].

The proposed control scheme runs on the Jetson Xavier board. We tested at first the targeting system with 2D scenes virtual aphids (to isolate the targeting performance from the aphid detection one). We input in real-time the coordinates of virtual aphids randomly located in the images of the camera. We did the same to evaluate the performance of the system with moving targets, with varying coordinates of virtual aphids in the images. The camera was located on top of a 40 cm-radius disk that was explored by the visual servoing system with a low power laser beam (see Fig. 4). During experiments, the system orientated the micro-mirrors to make the laser spot, visible on the plane, travel as fast as possible to each target.

2.4.2. Multiple Target Optimization

When multiple pest targets are present in the image, optimization is required to minimize the global distance traveled and thus to reduce the time taken to destroy all the targets. An example of a popular algorithm in literature is the Traveling Salesman Problem (TSP). It is a combinatorial optimization algorithm that computes the shortest possible path to reach once a set of objects. However, the TSP literature mainly considers only stationary targets and ignores any time-dependent behavior, which is critical in this application since every target moves relative to the camera. It results in a delayed disappearance from the image and thus their potential miss. Helvig et al. [29] proposed a generalization of a time-dependent TSP, which they called Moving-Target TSP. It was related to several applications where a pursuer must intercept in a minimum time a set of targets moving with constant velocities. The following theorem was developed for a mixture of approaching and receding targets from the origin, which would be analogous to this application where aphids are
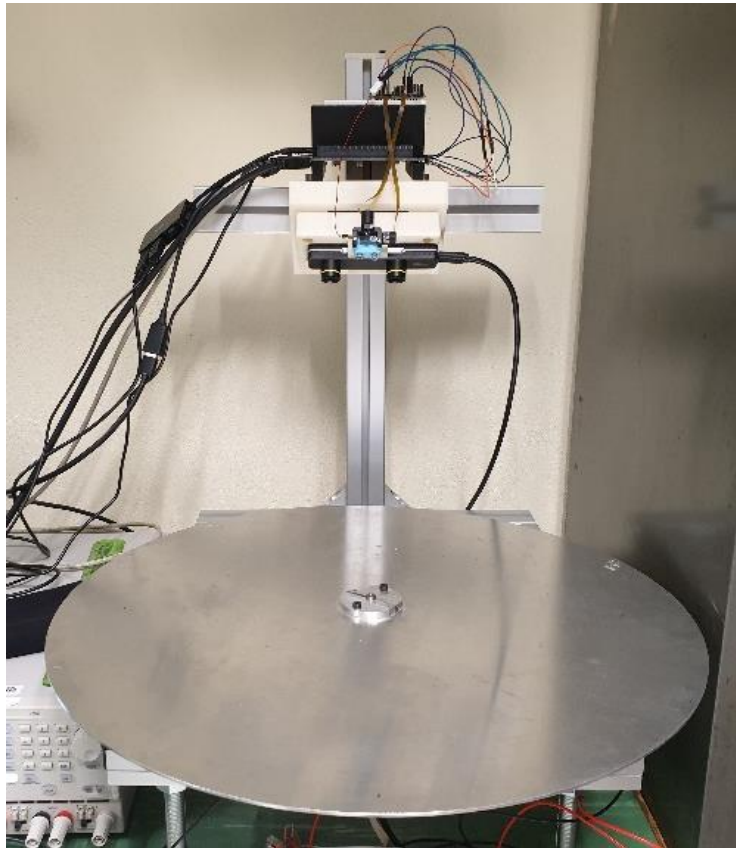
Figure 4. Visual-servoing experimental setup

approaching and receding the origin of the image. Two types of optimization algorithms were developed and tested:

- Moving-Targets TSP,
- Hybrid: Moving-Targets TSP and Nearest Neighbor.

The first one consisted in prioritizing the targets in the function of their distance to the image origin, in increasing order. This is equivalent to prioritizing the targets with the greatest Y-coordinate in the image axis (see Fig. 5). An alternative solution was tested where a secondary criterion was applied giving priority to the nearest target from the current position, selected among the lower-most targets.

To evaluate the performance of the system with moving targets, we made the virtual aphids translate (towards the bottom of the image) in real-time in the images at a constant velocity of 5 pixels per second. We also performed experiments with blue led stripes located in a 40 cm $\times$ 20 cm on a rotating disc, to test the system including some target detection. We could not use alive aphids as they constantly move in such a situation. We either could not use dead ones as they do not keep their initial color for enough time.
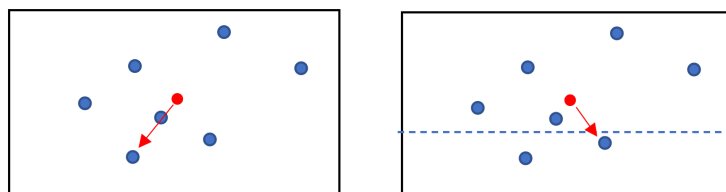

Figure 5. Representation of the Moving-Target TSP method (left) and the hybrid method with the added Nearest Neighbor variant.

2.5. Laser Choice and Dimensioning

To select the most effective laser, the correlation between laser energy and aphid mortality was evaluated and published in a previous work [30]. For this purpose, a first experiment to determine the Lethal Dose (LD) necessary to achieve a 90% mortality (LD90) at Day+1 was set up as in [31,32]. Three wavelengths have been used, each one covering a different part of the electromagnetic spectrum: 532nm (visible), 1090nm (Short Wavelength Infrared-SWIR), and 10.6μm (Long Wavelength Infrared-LWIR) known as a CO_2 laser, manufactured by CNI Lasers, IPG and Access Laser respectively. Samples of 48 aphids originating from the three lines aforementioned were used. The aphids were random unsynchronized adults, representative of what would be found in a field without an early detection system. The Hosmer-Lemeshow test and the "area under the Receiver Operating Characteristic curve" test were performed on logistical fits to ensure that the retrieved fit was correct and accurate.

Then, to analyze the mortality dynamics of aphids during their development, the same experiment was conducted on synchronized one-day-old nymphs (N1) with a mortality counting every day until they reached their adult stage on the 7th day, thus considering an LD90 at Day+7. Given the great results of the previous experiment, we focused on the 10.6μm laser and used the *A.pisum* line LL01 so we could rely on their well-known life-history traits [33].

Going further, potential transgenerational laser-induced effects have been addressed as well. To do this, we reproduced the previous experiment, but this time using an LD50 to have a good balance between the number of survivors and quantifiable laser-induced effects and to ensure a robust statistic. The survivors of irradiated aphids generation (F0) at Day+7 gave birth to nymphs of the second generation (F1) every day for 15 days. For the two generations F0 and F1, mortality was assessed every day during their development, then we measured their mass and developmental delay at Day+7. Finally, we monitored the fecundity for 15 days of F0 aphids and F1 aphids born on the 1st, 5th, 10th and 15th day of the reproduction period of F0 aphids [30]. The mortality rate of the synchronized N1 aphids is presented here with a GLM Gaussian test with a 95% confidence interval.

Moreover, the laser beam must be innocuous for host plants. Indeed, in case of false-positive detection, the entire laser energy would strike them. Hence, the impact of the energy delivered in our experiments has also been investigated on host plants in our previous work [30]. *Vicia Faba* and *Triticum aestivum* host plants, for respectively *A. pisum* and *R.padi* lines, were chosen. We shot the host plants 4 times with different values found in each experiment with the 10.6μm laser. First, to ensure no underestimation, we used the highest fluences corresponding to LD90 at Day+1 on *A. pisum* LL01 and *R. padi* adult aphids. Then, we also used the fluence that is the most reasonable for in-field use, corresponding to LD90 at Day+7 on N1 LL01 aphids. According to aphids' location on their host plants, we shot different organs namely the adaxial and abaxial leaf surfaces, the stem, and the apex. Samples of 20 plants were shot by fluence level and by targeted organ. On Day+7, height, fresh mass, and leaf surface were measured.

3. Results

A prototype has been designed and built with the only purpose to validate the localization-neutralization loop on a single seedlings row (see Fig. 6). The experimental results performed in laboratory with this prototype demonstrate the feasibility of detecting different lines of aphids (50% detected at 3 cm/s) and of neutralizing them without impacting the growth of their host plants.

3.1. Aphid Detection and Localization

3.1.1. Lighting Conditions

We could observe that the best results in aphid detection were obtained with the white LEDs. Hence, white LED strips have been installed into the robot to create a homogeneous lighting environment, reducing the sensibility to external conditions (see Fig 7). The camera
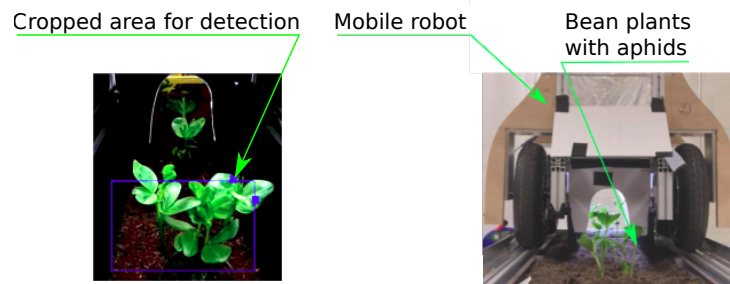
Figure 6. On the left image, a picture acquired by the camera of the mobile robot, only the area contained in the blue frame is analyzed. The blue squares indicate the location of the detected aphids. On the right image, the robot spans a row of broad bean plants featuring aphids (front view).

settings were also adjusted to limit light reflections and maximize the contrast (maximum contrast and saturation, reduced gain, see Table 1). These results were obtained with the robot over an artificial ground reproducing near field conditions. They should be confirmed by real in-field experiments with various natural ambian light conditions.
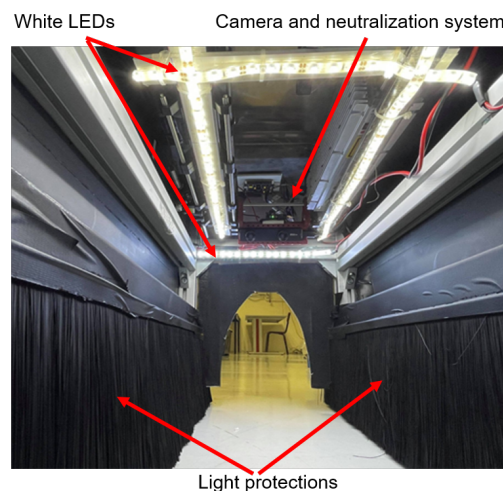

Figure 7. Under the robot: light sources and protections, camera and neutralization systems.

3.1.2. Localization Performance

Table 2 summarizes the experimental results obtained with both proposed networks. We manually optimized the UNet-HD architecture and its hyper parameters to obtain the best results in terms of true positive detection (TP). Such optimization was not performed on YOLO. Despite the manual optimization, YOLOv4 outperforms the UNet-HD network considering the speed, precision, and sensibility criteria. Therefore, we worked on the optimization of YOLO. The effect of cropping the camera images and keeping only the relevant area (800x800 pixels) led to a raise of 6% in accuracy and 5% in sensitivity compared to a whole picture. Indeed, the Yolo network has an input dimension of 512x512 pixels. Resizing the entire image (2208x1242 pixels) to 512x512 pixels blurred objects in the image and caused a reduction in precision.

To get better accuracy, we also tiled the area of 800x800 pixels into 4 or 16 sub-parts. The inference speed (frames per second) was computed when the network had ended up processing all these areas. We observed an increase in sensitivity when using 400x400 pixel tiles (0.73 versus 0.51 for 800x800 pixel tiles). In the case of very small images (200x200 pixels), the sensitivity falls to 0.53. We also noticed that this method greatly reduces the inference speed of the model because of the large number of images to be processed for each capture. We also observed that the code developed in C++ was more efficient than

	YOLOv4	UNet-HD
FPS (Nvidia Quadro 400)	**10-11**	2-3
True Positive (TP)	238	**278**
False Positive (FP)	**490**	997
False Negative (FN)	1371	**1349**
Precision	**0.37**	0.15
Recall	**0.21**	0.17

Table 2. Performance comparison between YOLOv4 and UNet with Hausdorff distance (UNet-HD) for aphid detection. Values in bold indicate the best results for each criterion.

that of API Python (about 1.5 times faster in terms of FPS speed). The averaged results on our test set are visible in table 3.

Network input size	Input image size	FPS (quadro 400)		Precision	Recall
		Python API	C++		
640x640	2208x1242	10-11	16	0.35	0.49
512x512	2208x1242	13-14	**21**	0.34	0.46
512x512	800x600	13-14	**21**	**0.4**	**0.51**

Table 3. Performance comparison for YOLOv4 with smaller images.

We were then able to double the model inference speed using the tkDNN engine, from 9 FPS to 19 FPS: more than our real-time detection expectations.Indeed, the detection module can rotate by itself from 90 to 100 frames per second with this library. Nevertheless, since the acquisition and detection processes are synchronized, the overall detection speed is restricted by the capture speed of the camera.

3.2. *Laser-based Neutralization*

3.2.1. Pest neutralization

The efficiency of the laser treatment on unsynchronized adult aphids is displayed in Fig. 8. Only results with the 532nm and 10.6μm lasers are introduced. Indeed, the 1090nm laser ended in being too much ineffective; it is not included in this paper's results for the sake of clarity. LD90 values are derived from the logistic fits in solid lines corresponding to experimental data points. For *A. pisum* LL01 (green) and YR2 (pink) aphids, the 10.6μm wavelength is more effective than 532nm. For instance, with green aphids, values of 53.55J.cm^{-2} and 12.91J.cm^{-2} are retrieved at 532nm and 10.6μm respectively. Indeed, going from one laser to another result in an LD90 more than four times lower. Hence, the 10.6μm wavelength has been chosen for the rest of the study. These values are quite the same for the pink aphids. However, this is not the case for *R. padi* (black) aphids. In this case, both wavelengths exhibit the same efficiency. The smaller size of this specie can explain this difference.

By changing the targeted aphid stage and extending the observation period, the LD90 can be loweù red again (Fig. 9a.). Consequently, a lower LD90 fluence means faster, more secure, and more energy-saving treatment. Thus, targeting nymphs results in an LD90 at Day+1 lowered by four times compared to adults. Moreover, counting the nymphs mortality at Day+7 instead of Day+1 leads to a 2.6 times decreased LD90 value. Globally, targeting nymphs and observing them at Day+7 allows for decreasing the fluence to 1.15J.cm^{-2}. This value is ten times lower than the previous while still maintaining a high level of 90% neutralization rate.

Moreover, according to Fig. 9b., the mortality dynamics of aphids over 7 days is not linear. Indeed, most aphids are already neutralized after 3 days and then a plateau is reached. This means that the LD90s at Day+7 and Day+3 are almost identical. Consequently,
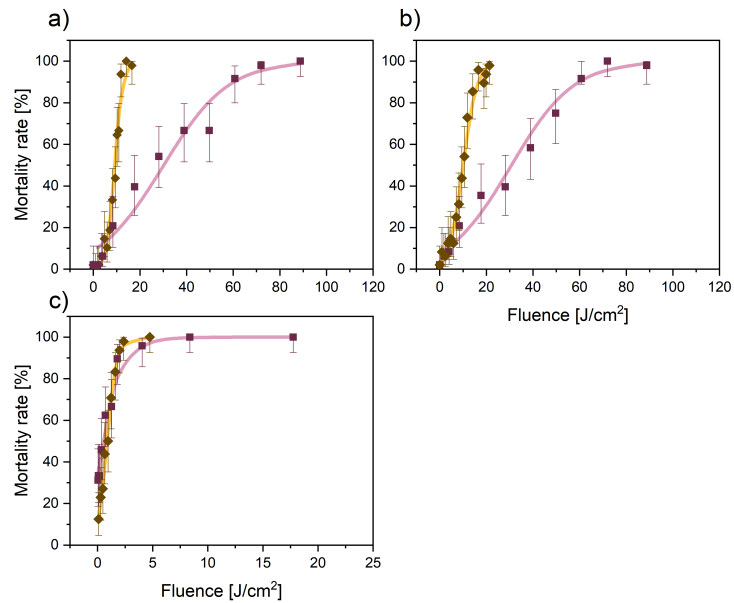
Figure 8. Mortality rate over the fluence for several aphid lines. Upper left : *A.pisum* LL01 (green aphids). Upper right : *A.pisum* YR2 (pink aphids). Lower left : *R.padi* LR01 (black aphids). Square and pink curve : 532nm experiment. Diamond and yellow curve : 10.6μm experiment. Curves represent logistic fits. Adapted from [30].

the irradiated aphids with a low fluence will already be dead after 3 days, thus reducing the duration of their attack on the plants.

Regarding potential transgenerational effects, results show that laser treatment does not induce any significant effect on the mortality of the next F1 generation (Fig. 9c.). Hence, the laser-based strategy must be based on direct laser effects.

3.2.2. Targeting

The IBVS algorithm featuring a PID controller obtained best results versus the two variants of AG. We could obtain a mean response time $t_{5\%}$ = 490 ms (versus 830 and 920 for AG), corresponding to a mean $t_{5\%}$ = 490 ms (see Fig 10). With moving virtual targets, the PID control showed slightly better performance with a mean $t_{5\%}$ = 420 ms (versus 590 and 870 for AG). We also performed experiments with velocities ranging from 5 to 12 pixels/s. We observed that the system did not have the time to travel to all targets at 12 pixels/s and over (corresponding approximately to 1 cm/s at a distance of 30 cm). Experiments with blue LED stripes showed a mean response time $t_{5\%}$ that greatly increased to 620 ms.

4. Discussion

Concerning the detection of aphids, by inferring with 2208x1242 pixel resolution images, we found that the speed of Hausdorff-optimized U-Net detection was not suitable for real-time application. As the images were captured at 15 FPS by the ZED mini camera and this network can process only 2 or 3 per second, many images were not taken into account when the robot was moving. This was due to the too high deepness of this model that was set to increase the ability to detect small objects. This was indeed a gain in precision but a loss in efficiency. Moreover, the accuracy of UNet was not better than that of YOLOv4 (accuracy 0.15 against 0.21 of YOLOv4) as it generated much false detection (997 false positives versus 490 false positives for YOLOv4). We then simplified the architecture of UNet by reducing the number of layers and by training it with cropped images of smaller size. However, its accuracy remained poor compared to the model of Darknet YOLOv4. The simplified UNet model failed to achieve 10% accuracy on cropped areas of 400x400
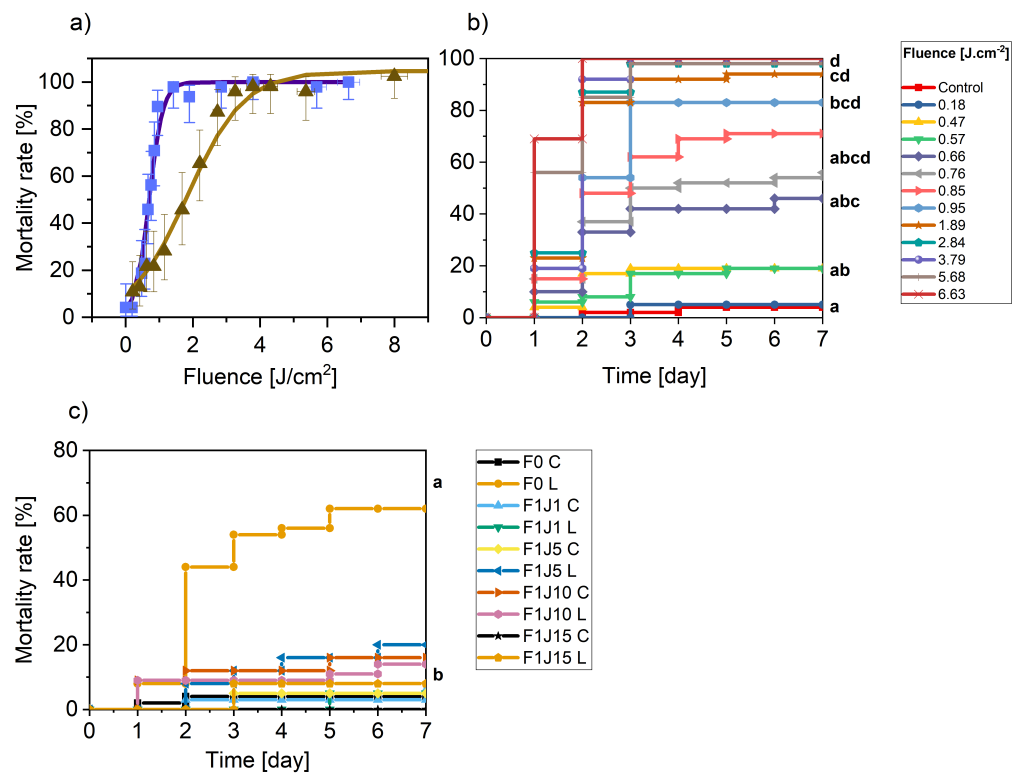
Figure 9. a) Mortality rate over the fluence for *A. pisum* LL01 (green) N1 aphids at Day+1 (triangle and brown curve) and Day+7 (square and blue curve). Error bars are plus and minus exact binomial 95% confidence intervals. b) Evolution of the mortality rate for several fluence using the 10.6μm laser on N1 *A.pisum* LL01 populations. c) Mortality rates over time for the first (F0) and second (F1) N1 *A.pisum* LL01 aphid generations. C letter refers to the untreated condition, while L letter refers to the irradiated one at F0. F1 JX refers to the second generation born the 1st, 5th, 10th and 15th day during the F0 reproduction period. Letters in the right refer to the results of the 95% confidence interval GLM Gaussian test. Adapted from [30].
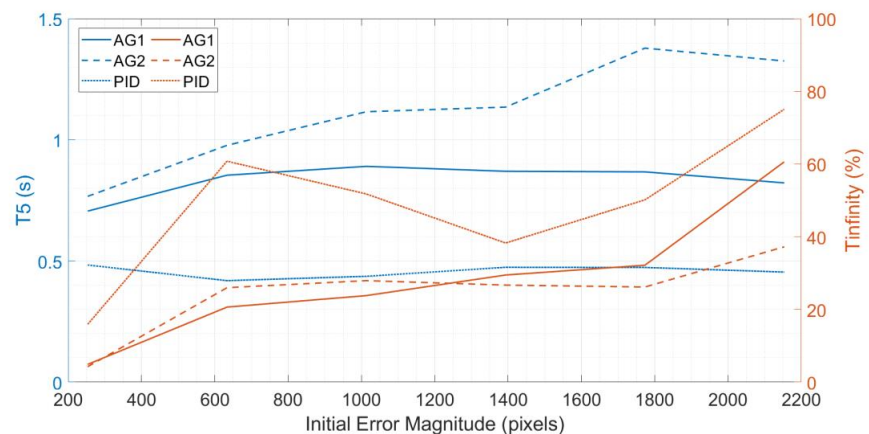

Figure 10. Evolution of $t_5\%$ and t_∞ response times versus initial error magnitudes for PID, AG1, and AG2 control laws.

pixels. Taking into account these results, we therefore decided to apply YOLOv4 for the detection of aphids, with aforementioned accuracy and speed optimizations.

We could obtain medium performance in 2D scenes with mean travel times of 620 ms between two targets. This is quite too low a value, that was obtained in perfect lab conditions with virtual aphids. With blue LED stripes, the bad results were due to some disturbance provided by the LEDs when the laser spot was very close to a LED. The detection algorithm had trouble distinguishing the laser spot from the neighbor LED. Even if we did not meet this issue with real aphids later on the real robot, plants infected with tens of aphids should be treated faster to enable a 1 ha field treatment in 24 h at 29 cm/s. Speed improvement speed should be researched or a robot spanning several rows with several detection/neutralization modules working in parallel. Faster micro-mirrors should be envisaged, taking into account the cost and affordability of such a robot.

Also, to perform a precise localization of the laser spot, it was necessary to be in a black ambiance while the aphid detection required a good luminosity. We then had to alternate both detection and synchronize the lighting so that each detection is performed in the best lighting conditions. In the robot, as we employ LED stripes, we could efficiently perform the switching, but these working conditions diminish the operational flow. On-robot experiments showed that the performance decreases as soon as the lighting conditions deteriorate and 3D objects are present in the scene, necessitating stopping the robot. Indeed, in 3D scenes, the spot was sometimes not visible due to the non-alignment of the laser source and the camera axis and the presence of leaves in different depths of field. The algorithm had to work blindly during the time the spot remains invisible. When this period was too long, the system skipped this target and selected the next one. This slowed much the servoing and reduced much the performance. Therefore, during the experiments, to decrease these periods, even if we could detect aphids with the robot moving, we preferred stopping it during the targeting phases. Moreover, performance decreases as soon as the lighting conditions deteriorate (which may be the case during sunny days with external rays of light coming through the entrance for plants) and 3D objects are present in the scene, necessitating stopping the robot. A study enhancing the robustness of visual servoing in the presence of occlusions is mandatory.

At last, Newscale micro-mirrors are too fragile for farming conditions. Other stronger solutions have to be studied, knowing that we did not study the impact of vibrations due to the locomotion of the robot on the ground yet.

Regrettably, we could not validate (for logistical reasons) the whole chain simultaneously (from aphid detection to neutralization with the power laser): detection / localization / targeting has been validated independently from targeting / neutralization. Globally, we could make the robot proceed at a velocity of 3cm/s and have it detect 50% of the present aphids, and then target 83% of the detected aphids, on 3 successive broad bean plants featuring each one with 8 aphids. It is clearly far from the requirements but it provides a first proof of concept validating the feasibility of such an approach.

Regarding aphid neutralization, we found that the CO_2 laser is best suited to neutralize almost all aphids with low fluences by raising their cell water temperature with LWIR at 10.6μm. Indeed, the energy needed to have an LD90 after one day in an adult population equal to 12.91J.cm^{-2} per shot was 4 times lower than the other lasers tested. Additionally, targeting younger aphids as N1 and extending the observation period by a few days can lower 10 times the energy required, resulting in 1.15J.cm^{-2}. These results and our estimates of energy consumed for a field treatment detailed in our previous work [30] show that the laser is not the most power-consuming component in our robot. However, the detection must be very precise to target aphids at the youngest stages and to differentiate them from other insects beneficial to crops. Moreover, because most aphids are localized on the abaxial leaf surface, the optical chain must be adjusted to be able to target aphids on leaves from below. Finally, in case of a false positive detection, we made sure that hitting leaves wouldn't impact the plant growth [30].

5. Conclusions

The experimental results globally demonstrate, in lab conditions, the feasibility of detecting different lines of aphids (50% detected at 3 cm/s) and of neutralizing them by CO_2 laser shots with high efficiency (90% mortality after 3 days with 1.15J.cm^{-2} for *A.pisum* LL01 N1) without impacting the growth of their host plants in case of missed shot. Showing the feasibility of this approach is encouraging as aphids are one of the most difficult crop pests to combat. However, aphids neutralization is closely dependent on the quality of the detection, since it is recommended to detect aphids at the nymphal stage and to differentiate them from the beneficial insects that one wishes to preserve on the crops. Other pests such as fall armyworms *Spodoptera frugiperda* and dark sword grass *Agrotis ipsilon larvae* that are bigger should pose fewer detection issues. Future directions consist in enhancing the performance of the detection and targeting phases to get characteristics closer to the requirements making it useful in a real farming context. Also, the robustness concerning field conditions is to be studied. The most worrying aspect is the presence of vibrations due to the irregular ground that may decrease the performance of the positioning of the micro-mirrors and so the quality of the pest targeting.

Author Contributions: Conceptualization, A.H., A.L., B.M., F.G.F., K.R., P.D.S., M.T.P., R.M., T.G., and V.L. ; methodology, A.L., B.M., F.G.F., K.R., M.T.P., P.D.S., R.M., S.P., T.G., and V.L. ; software, J.D.S., T.N., V.D., and V.N., ; validation, A.L., B.M., F.G.F., K.R., M.T.P., P.D.S., R.M., S.P., T.G., V.L., and V.N.; formal analysis, B.M., K.R., M.T.P., P.D.S., R.G., R.M., S.P., T.N., and V.L.; investigation, F.G.F., J.D.S., R.G., S.P., T.N., V.D., V.L., and V.N. ; resources, K.R., V.D., V.L., and S.P.; data curation, J.D.S., R.G., S.P., V.D., and V.L.; writing—original draft preparation, A.L., B.M., F.G.F., J.D.S., K.R., M.T.P., P.D.S., R.M., R.G., S.P., T.G., T.N., V.D., V.L., and V.N.; writing—review and editing, A.L., B.M., K.R., M.T.P., P.D.S., R.G., R.M., S.P., T.G., and V.L.; visualization, J.D.S., K.R., P.D.S., R.G., S.P., T.G., V.D., and V.L.; supervision, A.L., B.M., F.G.F., K.R., M.T.P., P.D.S., R.M., and T.G.; project administration, A.H., A.L., B.M., F.G.F., and K.R.; funding acquisition, A.H., A.L., B.M., F.G.F., and K.R.All authors have read and agreed to the published version of the manuscript.

Funding: This research was funded by ANR grant number ANR-17-CE34-0012.

Data Availability Statement:

Acknowledgments:

Conflicts of Interest: The authors declare no conflict of interest.

Abbreviations

The following abbreviations are used in this manuscript:

MDPI	Multidisciplinary Digital Publishing Institute
DOAJ	Directory of open access journals
TLA	Three letter acronym
LD	Linear dichroism

References

1. RISE Foundation. Crop Protection & the EU Food System: Where are they going? v1, 2020.
2. Pesticide Action Network Europe. Endocrine Disrupting Pesticides in European Food, 2017.
3. Tang, F.H.M.; Lenzen, M.; McBratney, A.; Maggi, F. Risk of pesticide pollution at the global scale. *Nature Geoscience* **2021**, *14*, 206–210.
4. Ellis, C.; Park, K.J.; Whitehorn, P.; David, A.; Goulson, D. The Neonicotinoid Insecticide Thiacloprid Impacts upon Bumblebee Colony Development under Field Conditions. *Environmental Science & Technology* **2017**, *51*, 1727–1732, [https://doi.org/10.1021/acs.est.6b04791]. PMID: 28079366, https://doi.org/10.1021/acs.est.6b04791.
5. Saiz-Rubio, V.; Rovira-Más, F. From Smart Farming towards Agriculture 5.0: A Review on Crop Data Management. *Agronomy* **2020**, *10*. https://doi.org/10.3390/agronomy10020207.
6. Vougioukas, S.G. Agricultural Robotics. *Annual Review of Control, Robotics, and Autonomous Systems* **2019**, *2*, 365–392, [https://doi.org/10.1146/annurev-control-053018-023617]. https://doi.org/10.1146/annurev-control-053018-023617.
7. Žibrat, U.; Knapič, M.; Urek, G. Plant pests and disease detection using optical sensors/Daljinsko zaznavanje rastlinskih bolezni in škodljivcev. *Folia biologica et geologica* **2019**, *60*, 41–52.

8. Mahlein, A.K.; Kuska, M.T.; Behmann, J.; Polder, G.; Walter, A. Hyperspectral sensors and imaging technologies in phytopathology: state of the art. *Annual review of phytopathology* **2018**, *56*, 535–558.
9. Johnson, J.B.; Naiker, M. Seeing red: A review of the use of near-infrared spectroscopy (NIRS) in entomology. *Applied Spectroscopy Reviews* **2020**, *55*, 810–839, [https://doi.org/10.1080/05704928.2019.1685532]. https://doi.org/10.1080/05704928.2019.1685532.
10. Martineau, M.; Conte, D.; Raveaux, R.; Arnault, I.; Munier, D.; Venturini, G. A survey on image-based insect classification. *Pattern Recognition* **2017**, *65*, 273–284. https://doi.org/https://doi.org/10.1016/j.patcog.2016.12.020.
11. Xie, C.; Wang, H.; Shao, Y.; He, Y. Different algorithms for detection of malondialdehyde content in eggplant leaves stressed by grey mold based on hyperspectral imaging technique. *Intelligent Automation & Soft Computing* **2015**, *21*, 395–407.
12. Li, R.; Wang, R.; Xie, C.; Liu, L.; Zhang, J.; Wang, F.; Liu, W. A coarse-to-fine network for aphid recognition and detection in the field. *Biosystems Engineering* **2019**, *187*, 39–52.
13. Obasekore, H.; Fanni, M.; Ahmed, S.M. Insect Killing Robot for Agricultural Purposes. In Proceedings of the 2019 IEEE/ASME International Conference on Advanced Intelligent Mechatronics (AIM), 2019, pp. 1068–1074. https://doi.org/10.1109/AIM.2019.8868507.
14. Wu, X.; Aravecchia, S.; Lottes, P.; Stachniss, C.; Pradalier, C. Robotic weed control using automated weed and crop classification. *Journal of Field Robotics* **2020**, *37*, 322–340, [https://onlinelibrary.wiley.com/doi/pdf/10.1002/rob.21938]. https://doi.org/https://doi.org/10.1002/rob.21938.
15. Kaierle, S.; Marx, C.; Rath, T.; Hustedt, M. Find and Irradiate — Lasers Used for Weed Control. *Laser Technik Journal* **2013**, *10*, 44–47, [https://onlinelibrary.wiley.com/doi/pdf/10.1002/latj.201390038]. https://doi.org/https://doi.org/10.1002/latj.201390038.
16. Asha, K.; Mahore, A.; Malkani, P.; Singh, A.K. Robotics-automation and sensor-based approaches in weed detection and control: A review. *International Journal of Chemical Studies* **2020**, *8*, 542–550.
17. Fuad, M.T.H.; Fime, A.A.; Sikder, D.; Iftee, M.A.R.; Rabbi, J.; Al-Rakhami, M.S.; Gumaei, A.; Sen, O.; Fuad, M.; Islam, M.N. Recent Advances in Deep Learning Techniques for Face Recognition. *IEEE Access* **2021**, *9*, 99112–99142. https://doi.org/10.1109/ACCESS.2021.3096136.
18. Minaee, S.; Boykov, Y.; Porikli, F.; Plaza, A.; Kehtarnavaz, N.; Terzopoulos, D. Image Segmentation Using Deep Learning: A Survey. *IEEE Transactions on Pattern Analysis and Machine Intelligence* **2022**, *44*, 3523–3542. https://doi.org/10.1109/TPAMI.2021.3059968.
19. Minks, A.K.; Harrewijn, P. *Aphids: their biology, natural enemies, and control*; Elsevier, 1987. OCLC: 13360853.
20. Bochkovskiy, A.; Wang, C.Y.; Liao, H.Y.M. Yolov4: Optimal speed and accuracy of object detection. *arXiv preprint arXiv:2004.10934* **2020**.
21. Wang, C.Y.; Liao, H.Y.M.; Yeh, I.H.; Wu, Y.H.; Chen, P.Y.; Hsieh, J.W. CSPNet: A New Backbone that can Enhance Learning Capability of CNN, 2019. https://doi.org/10.48550/ARXIV.1911.11929.
22. Liu, S.; Qi, L.; Qin, H.; Shi, J.; Jia, J. Path Aggregation Network for Instance Segmentation, 2018. https://doi.org/10.48550/ARXIV.1803.01534.
23. Schubert, E.; Sander, J.; Ester, M.; Kriegel, H.P.; Xu, X. DBSCAN Revisited, Revisited: Why and How You Should (Still) Use DBSCAN. *ACM Trans. Database Syst.* **2017**, *42*. https://doi.org/10.1145/3068335.
24. Hutchinson, S.; Hager, G.; Corke, P. A tutorial on visual servo control. *IEEE Transactions on Robotics and Automation* **1996**, *12*, 651–670. https://doi.org/10.1109/70.538972.
25. Andreff, N.; Tamadazte, B. Laser steering using virtual trifocal visual servoing. *The International Journal of Robotics Research* **2016**, *35*, 672–694, [https://doi.org/10.1177/0278364915585585]. https://doi.org/10.1177/0278364915585585.
26. Kudryavtsev, A.V.; Chikhaoui, M.T.; Liadov, A.; Rougeot, P.; Spindler, F.; Rabenorosoa, K.; Burgner-Kahrs, J.; Tamadazte, B.; Andreff, N. Eye-in-Hand Visual Servoing of Concentric Tube Robots. *IEEE Robotics and Automation Letters* **2018**, *3*, 2315–2321. https://doi.org/10.1109/LRA.2018.2807592.
27. Keller, M.D.; Norton, B.J.; Farrar, D.J.; Rutschman, P.; Marvit, M.; Makagon, A. Optical tracking and laser-induced mortality of insects during flight. *Scientific Reports* **2020**, *10*, 14795.
28. Lagadic team. ViSP Tutorial: How to boost your visual servo control law, 2021. Accessed Apr. 28, 2021.
29. Helvig, C.S.; Robins, G.; Zelikovsky, A. Moving-Target TSP and Related Problems. In Proceedings of the Algorithms — ESA' 98; Bilardi, G.; Italiano, G.F.; Pietracaprina, A.; Pucci, G., Eds.; Springer Berlin Heidelberg: Berlin, Heidelberg, 1998; pp. 453–464.
30. Gaetani, R.; Lacotte, V.; Dufour, V.; Clavel, A.; Duport, G.; Gaget, K.; Calevro, F.; Da Silva, P.; Heddi, A.; Vincent, D.; et al. Sustainable laser-based technology for insect pest control. *Scientific Reports* **2021**, *11*, 11068. https://doi.org/10.1038/s41598-021-90782-7.
31. Keller, M.D.; Leahy, D.J.; Norton, B.J.; Johanson, T.; Mullen, E.R.; Marvit, M.; Makagon, A. Laser induced mortality of Anopheles stephensi mosquitoes. *Scientific Reports* **2016**, *6*. https://doi.org/10.1038/srep20936.
32. Hori, M.; Shibuya, K.; Sato, M.; Saito, Y. Lethal effects of short-wavelength visible light on insects. *Scientific Reports* **2015**, *4*, 7383. https://doi.org/10.1038/srep07383.
33. Simonet, P.; Duport, G.; Gaget, K.; Weiss-Gayet, M.; Colella, S.; Febvay, G.; Charles, H.; Viñuelas, J.; Heddi, A.; Calevro, F. Direct flow cytometry measurements reveal a fine-tuning of symbiotic cell dynamics according to the host developmental needs in aphid symbiosis. *Scientific Reports* **2016**, *6*, 19967. https://doi.org/10.1038/srep19967.